Hindawi
Journal of Nanomaterials
Volume 2023, Article ID 5440142, 7 pages
https://doi.org/10.1155/2023/5440142

Research Article

Influence of SiO_2 Filler Addition on the Types I and II Shear Fracture Toughness of Hemp Fiber-Reinforced Epoxy Mixtures

L. Natrayan,[1] Raviteja Surakasi,[2] M. S. Heaven Dani,[3] Pravin P. Patil,[4] T. Manikandan,[5] K. Tamil Mannan,[6] and Muse Degefe Chewaka[7]

[1]*Department of Mechanical Engineering, Saveetha School of Engineering, SIMATS, Chennai 602105, Tamil Nadu, India*
[2]*Department of Mechanical Engineering, Lendi Institute of Engineering and Technology, Jonnada, Vizianagaram 535005, Andhra Pradesh, India*
[3]*Department of Mechanical Engineering, Velammal Institute of Technology, Chennai 601204, Tamil Nadu, India*
[4]*Department of Mechanical Engineering, Graphic Era Deemed to be University, Bell Road, Clement Town, Dehradun 248002, Uttarakhand, India*
[5]*Department of Aeronautical Engineering, Nehru Institute of Technology, Coimbatore 641105, Tamil Nadu, India*
[6]*Department of Mechanical Engineering, School of Engineering and Technology, Indira Gandhi National Open University, Maidan Garhi, New Delhi 110068, India*
[7]*Department of Mechanical Engineering, Ambo Institute of Technology-19, Ambo University, Ambo, Ethiopia*

Correspondence should be addressed to Muse Degefe Chewaka; muse.degefe@ambou.edu.et

Received 5 August 2022; Revised 5 October 2022; Accepted 14 October 2022; Published 6 February 2023

Academic Editor: S. K. Khadheer Pasha

Natural fiber composites are now more costly than traditional building materials. Currently, industries are moving from traditional materials to natural fiber composites, and the price of natural fiber should be reduced through greater utilization of industrial production. This work aims to determine how matrix alteration affects the interlaminar characteristics of a hemp fiber-reinforced epoxy composite containing nano silicon oxide particles. Interlaminar modulus of rupture in Types I and II is assessed using dual cantilevered beams and end-notched deformation testing samples. Mechanical mixing and sonication are used to blend nanoscale SiO_2 (30 nm) into the resin at concentrations of 0, 0.2, 0.4, and 0.6 wt%. The composites were made using the compression molding method. The composites were tested according to the American Society for Testing and Materials standards after manufacturing. The findings show that adding nanoparticles enhances interlaminar toughness values. Interlaminar fracture toughness improved by 20.25% and 30.35% for 0.4 wt% SiO_2, respectively. The fiber matrix interaction and failure causes are examined using scanning electron microscope images.

1. Introduction

Recent advancements in lightweight materials suggest that natural fiber reinforcement in polymeric materials is becoming more popular. Because of increased international awareness and stricter environmental regulations, manufacturers focused primarily on eco-friendly materials [1]. Natural fibers have become popular for nonstructural and semistructural industries, resulting in environmental and financial gains over synthetic materials, as well as their least expensive, specific strength, and higher hardness. Natural fiber composites are widely utilized as reinforcement in composite materials, such as automobile cabins, interior doors, reporting tools, and sports gear, thanks to their features [2, 3]. Renewables should be chosen to create 10% of biochemical construction blocks by 2020, and that figure must be expanded to 50% by 2050, according to the US Departments of Agriculture and Energy. Cotton, coir, jute, flax, hemp, banana fiber, and other natural fibers are well-known for their use in automobile materials [4, 5]. Hemp has a particular strength and modulus that are equivalent to man-made glass fibers when compared to other natural fibers. If rigidity and lightness are taken into account, hemp is an excellent replacement for man-made fibers [6]. Hemp fibers are well-known for their use in the aviation, vehicle, building, recreation, sports, and package industries. Because of its likeness to the marijuana plant, its effects are frequently misconstrued [7, 8].

Medical cannabis can be grown in warm climatic regions on a variety of well-drained, upgradable soils that have high production and also no chemical fertilizer or herbicides, resulting in a height of 2–25 cm as well as a surface area of 3–5 cm. Because of its elevated hygroscopicity and organic material subject matter, this same cannabidiol seed is indeed a reduced farm physiologic epilog [9, 10]. With such an indigestible fiber interaction and greater configurability, treatment systems can produce premium cannabidiol natural fibers. Hemp fibers are encased in a hemicellulose and lignin matrix and arranged in a variety of architectural topologies. The architecture of hemp fibers has been widely investigated, resulting in helpful, in-depth information being available in the current literature [11, 12]. Hemp fibers are longer, stronger, and tougher than other plant materials like silk, as well as coarser, and are employed in engineering industries. As a consequence, composites (airline industry, sporting goods, etc.), structural and construction materials, geotextiles, and other applications account for approximately a quarter of the marijuana fibers used in commercial operations [13]. Hemp fibers take on a range of shapes, thicknesses, topologies, and properties during the course of their lives.

The watery characteristics of plant fibers and the hydrophobicity of epoxy matrix combine to make natural fiber composites' fiber matrix binding weak, resulting in poor mechanical characteristics and quick debonding failures. Debonding failures in fiber-reinforced composites are a key stumbling block to their widespread use [14]. Fibre interventions (alkali processing, ionized treatment), fiber modification, and matrix modification via nanoparticle inclusion are some of the methods used to address these drawbacks [15, 16]. These techniques provide a coarser fiber or matrices interface, which improves the mechanical connection of the fiber matrices, leading to an improved characteristic. When constructing composites for construction purposes, the resilience of the fiber and the matrix area to fracture progression is critical [16]. Matrix hardening makes fracture development parallel to a fiber orientation easier to control. Moreover, it makes a major contribution to the enhancement of lattice characteristics [17].

One technique to increase the hardness of the matrices and the fiber–matrix interaction is to add second-stage reinforcements to a matrix. When appropriately blended into the matrices, a tiny quantity of nanoparticles can considerably enhance the bulk characteristics of the material, like composite durability, rigidity, interfacial dimensional stability, mechanical characteristics, electrical characteristics, and thermal characteristics [18, 19]. Silicon, nano titanium dioxide, Al_2O_3, silicon dioxide, nanoclay, and other forms of second-stage reinforcement are used for matrices alteration in fiber-reinforced composites. Previous research on biocomposites has only looked at endurance, fabric pretreatment, fiber length, water uptake capabilities, and biomechanical qualities, including tension, bending, and impacts [20, 21]. The impact of adding nanoparticles to the matrix to increase mechanical characteristics and adhesive connections has received a little attention in academic nonfiction. Fernández-Álvarez et al. [22] and Guo et al. [23] studied the impacts of nanoparticles inclusion on *Hibiscus cannabinus*-based composites and found that at 3 wt% reinforcing load, the ductile and impression strength values improved by 25.80% and 29.81%, respectively. The explanation for the enhancement is the stronger interface connection formed between the matrix and the fiber. In cellulosic fiber composites, Thangaraj et al. [24] and Singh et al. [25] addressed the use of nanoscale silicon fillers. The modulus of elasticity, elastic strength, and toughness were all increased by 14.40%, 7.50%, and 6.10%, respectively. Nanosilicon offers a strong mix of qualities, like nontoxic, better interface with matrices, rust, and stability, among numerous second-stage reinforcements employed. SiO_2 is a naturally present silicon oxide that has attracted considerable attention due to its unique architectural, physiological, electrical, photonic, enzymatic, electrical, and anticorrosive properties [24, 25]. Chemicals' insolubility, cheap price, excellent adhesion with other substances, and a strong index of refraction all attract interest. Such properties of nanosilica contribute significantly to their selection as a good second-stage reinforcement element for polymer matrix, thereby improving the mechanical properties of fiber composites [26, 27].

Figure 1: Photographic images of reinforcement, filler, and matrix materials.

The purpose of this study is to determine the interfibrillar fracture toughness of unaltered and matrices-altered hemp fiber-reinforced composite materials in Types I and II. The inclusion of nanosilica into the matrices is used as a matrix alteration approach. The crack growth resistant curve is used in the Type I results to provide information on crack nucleation and crack growth toughness. The fracture starting rates for shearing type interfacial failures are also provided by the Type II findings. Scanning electron microscope (SEM) was used to evaluate the broken surfaces of the delaminated composite.

2. Experimental Works

2.1. Materials. The woven hemp fibers came from the Natural Fiber Industry in Vellore, Tamil Nadu, India (Stage I reinforcement). The hemp fibers were gently laved with clean water and sundried for 2 days to remove the moisture. The fiber was then immersed in the NaOH solution for 4 hr. The fabric was then cleansed in clean water before being woven at 75°C. As a matrix, silicon oxide and epoxy were employed in this study. Naga Pharmaceutical Manufacturing, Chennai, Tamil Nadu, India, provided the matrix and silicon oxide fillers (Stage II reinforcement). Figure 1 shows the photographic images of reinforcement and matrix materials. Table 1 reveals the common properties of fiber and matrix.

2.2. Fabrication of Nanocomposites. A stainless-steel mold measuring 300 mm × 300 mm × 3 mm was first refined. To generate a suitable matrix system, the matrix material was thoroughly combined with the hardener. The composite was

Table 1: Common properties of fibre and matrix.

Sr. no.	Properties	Hemp fiber	Epoxy resin
1	Cellulose (%)	67.4–69.18	–
2	Hemicellulose (%)	11–15.32	–
3	Lignin (%)	3.21	–
4	Density (g/cm^3)	1.37	1.21
5	Tensile strength (MPa)	279–862	7–21
6	Young's modulus (GPa)	69–70	0.88
7	Elongation (%)	2.3–3.18	1.54

made from hemp/nanosilica combinations using the compression molding process. Various weight percentages of nanosilicon powder (0, 0.2, 0.4 and 0.6 wt%) were dispersed in the manufactured epoxy by hand stirring with a glass rod. To avoid any shrinkage that may have happened during the extraction technique, the composite was cooled in the open air for several minutes. For the simple recovery of laminated composites, a mold release reagent was added to the steel mold. To guarantee appropriate soaking, the layers of hemp fibers were manually placed and resin was evenly sprayed on all the fibers. A high-temperature polymeric film was put between different layers of hemp fibers to create an interfacial precrack. Carbon fiber layers were put on both sides of the main hemp fiber layers to prevent mixed fracture formation due to significant beam deformation. The mold was then put on a heated compression molding equipment for 40 min at 120°C and 5 MPa pressure. The unaltered and matrices-altered hemp fiber composite structures are then cured at 90°C for 3 hr and 130°C for 1 hr in two stages.

2.3. Characterization of Nanocomposites. Type I interfacial fracture toughness tests were conducted using double cantilever beam test specimens in accordance with American Society for Testing and Materials (ASTM) D5528-13 guidelines. The test samples are 150 mm in length, 25 mm in breadth, and 3 mm in thickness. Aluminum plates with dimensions of 30 mm × 25 mm × 22 mm were bonded toward both sides of the specimens to keep the debonding length at 50 mm. To track the debonding process, a tiny piece of corrective liquid was applied to one side of the sample with a 1 mm marker. The specimen (Type II) was also exposed to a shearing failure mode. Using specimen specifications of 140 mm length, 25 mm breadth, and 3 mm thickness, five samples were evaluated under every test. With a cross-head movement of 0.5 mm/min, the test circumstances matched ASTM D7905-14 guidelines at the subatomic scale, SEM has been employed to start investigating broken lightweight structures. The samples had been washed, left to dry, as well as pretreated to nanometers of precious metals before SEM clarification to enhance the conductivities of the blends.

3. Results and Discussion

3.1. Type I Interlaminar Breakage Robustness. In Type I, the interfacial breakage robustness of hemp fiber-based lightweight material and matrices-altered specimens with nano-SiO_2 inclusion is investigated. The debonding behavior of the composites is represented by the force versus displacement

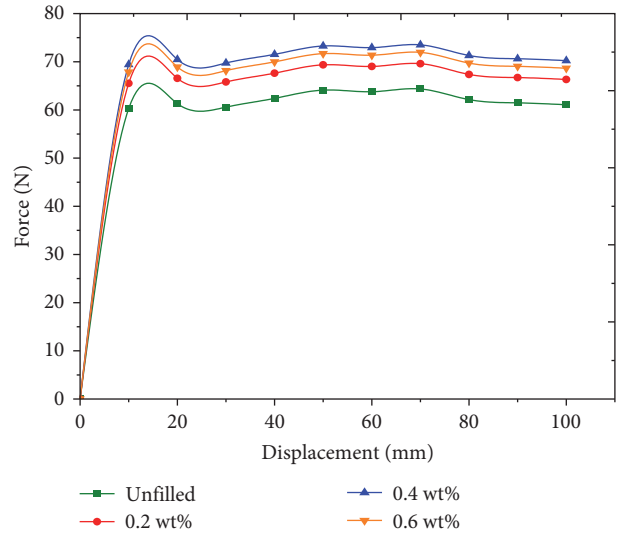

Figure 2: Force versus displacement curve of different weight ratios of nano-SiO_2 filler for Type I fracture.

graph in Figure 2. The curvature follows a clear structure until it reaches the maximum force line, which is the fracture starting point [28]. Further than that threshold, the force exhibits a drop that represents fracture development as the elongation rises. As the elongation progresses, force values increase and decrease in a stick–slip pattern [29]. This describes the fracture development trend in the composite's interfacial regions. The stick–slip pattern is most commonly seen in fabric when the material is delaminating. Moreover, the matrices' width in the hydrogen embrittlement axis is not consistent due to the transverse and longitudinal weaving patterns. As the fracture spreads, it encounters the areas of different hardnesses. Additional energy is stored in high-toughness areas till it achieves the requisite level to advance the fracture [30]. The stored energy from the tougher section is discharged as the fracture develops, causing the fracture to proliferate along the less hard zone, resulting in a sliding behavior. The abrupt force decreases or regions of uneven crack formation cause the slippage zones inside the force versus displacement curve [31].

The extensive experiments were consistent with those reported by Velmurugan and Babu [4] in weaved fiber composites. While comparing the matrices-altered composite to the baseline specimens, the matrices-altered composite had higher high force levels. The increase in force indicates that the latter is much more resistant to fracture progression, which is aided by the nanoparticle inclusion (up to 0.4 wt%). The decrease in force measurements for specimens with 0.6 wt% SiO_2 particle inclusion could be attributed to nanoparticle aggregation. Figure 3 shows the above findings.

3.2. Type II Interlaminar Breakage Robustness. In Type II, interfacial breakage robustness tests are performed on hemp fiber composites and matrices-altered composite specimens with silica inclusion at 0.2, 0.4, and 0.6 wt%. This is clearly shown in Figure 4. Shear load is added to ENF test specimens at the fracture start film. Microcracks form before the

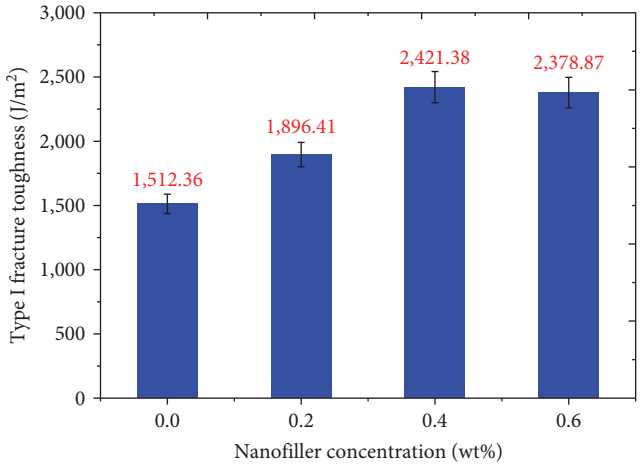

Figure 3: Fracture toughness values of different weight ratios of nano-SiO_2 filler for Type I fracture.

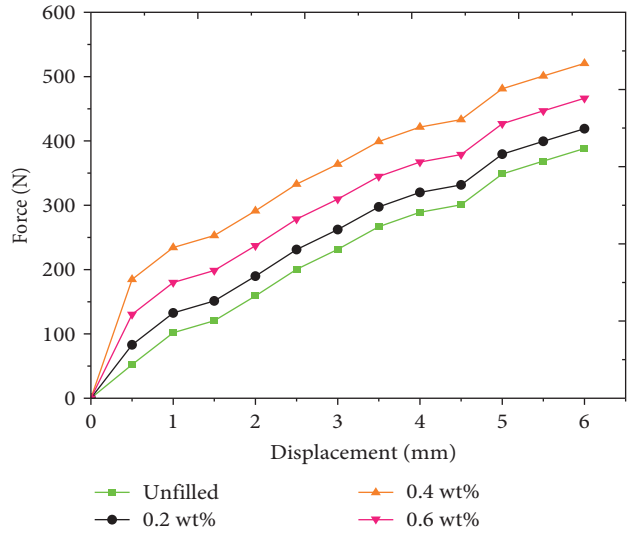

Figure 4: Force versus displacement curve of different weight ratios of nano-SiO_2 filler for Type II fracture.

crack tip. The microcrack expands and eventually combines as the load applied rises [32]. Crack growth begins at this point, and the load lowers abruptly shortly after attaining the highest load value [25]. In calculated Type II, interfacial brittle material values are calculated using the appropriate load capacity value. The fiber bridge technology is lacking in the Type II test. Beginning toughness is the name given to Type II toughness. The conformance calibration method is used, and the conformance results for all of the specimens are examined [33]. Figure 4 demonstrates the force versus displacement curves for unaltered and matrices-altered specimens, with 0.6% displaying the highest force values. Figure 5 shows the interfacial breakage robustness values for Type II. The unfilled or empty specimen has a Type II interfacial fracture toughness value of 1,812 J/m^2. Among them, 0.4 wt% showed the greatest increase in values (2,721 J/m^2), increasing by 33.40%. The existence of hackles and roughness between layers exposed to debonding are the factors that contribute to Type II interfacial fracture

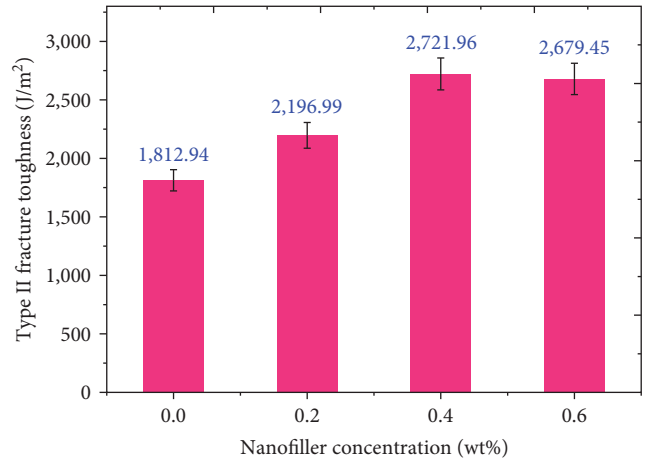

Figure 5: Fracture toughness values of different weight ratios of nano-SiO_2 filler for Type II fracture.

toughness levels. The addition of nano-SiO_2 to the matrices renders the lattice area harder [34].

During the operation of shear load on matrices-altered specimens, the enhanced interaction with the friction coefficient between interfacial layers avoids debonding. Through mechanical binding, the inclusion of second-stage reinforcements improves the interlock of the fiber matrices. When compared to unaltered composites, debonding failure occurs at a greater load level. The inclusion of nanosilica in the matrices makes the interface course, which helps to enhance the contact between fibers. As a result, the residual stress for the changed specimens is postponed. The van der Waals force acting among nanofillers causes nanomaterial aggregation at a greater weight percentage (beyond 0.4 wt%) of nanosilica in the matrices. The aggregates act as maximum stress points, causing the sample to fail at low stress. As a result, at greater weight percentages than 0.4 and 0.6 wt%, Types I and II interfacial fracture toughness values fall. The major effect of interface interaction among polymeric matrix, nanoparticles, and fiber reinforcement is responsible for the improved outcomes. In regards to interfacial fracture toughness values, the Types I and II test results show an enhancement in the reinforcement and resin interaction. When Types I and II interfacial fracture toughness values are compared, Type II findings are shown to have a larger enhancement range. The nanoparticle contributes more to the shearing type of breakdown resistance. The presence of nanoparticles in the matrices increases the fiber and the matrix interaction, as well as the matrix's roughness and durability, requiring considerable impulse for fracture development.

3.3. Microstructural Examination. SEM was used to examine the cracked interfaces of the nanocomposite in order to determine the role of nano-SiO_2 in interfacial fracture processes. At Satyabhama University, Tamil Nadu, a Zeiss SUPRA 55-VP SEM was employed to undertake microscopic assessments on cracked nanocomposites. To enhance the electrical properties of the nanocomposite, the samples were thoroughly washed, left to dry, and the outer layer was encased with 10 nm of gold prior to SEM analysis. During Type I test circumstances,

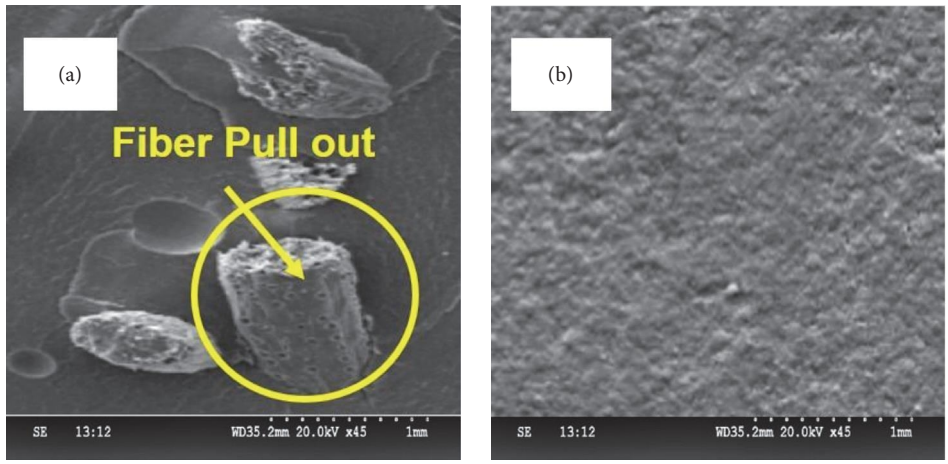

Figure 6: Microstructural images of Type I fracture: (a) unfilled composites; (b) 0.4 wt% nanosilica-based composite.

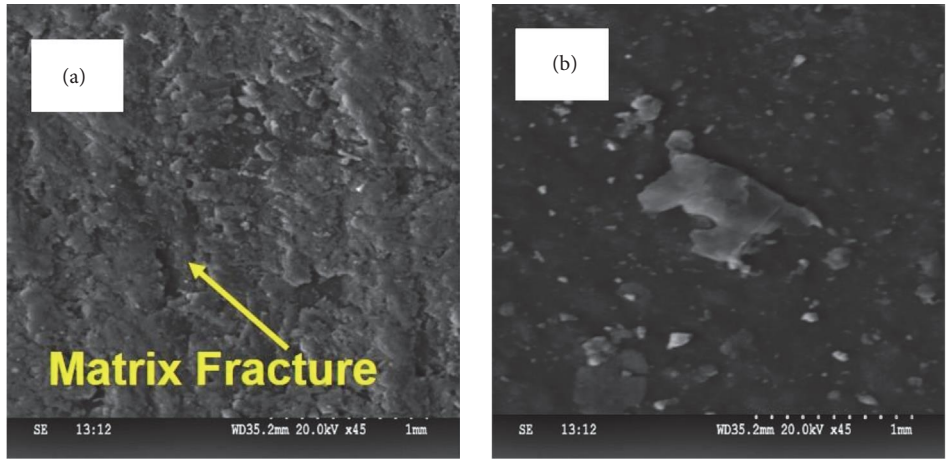

Figure 7: Microstructural images of Type II fracture: (a) unfilled composites; (b) 0.4 wt% nanosilica-based composite.

SEM micrographs of the cracked interface of the standard (unaltered matrices) and matrix-altered composite with nanosilica additions (0.2, 0.4, 0.6 wt% loaded) are shown in Figure 6. A neat and brittle form of breakdown between fiber matrix areas may be seen on the delaminated surfaces of the reference composite. Fiber interfaces can be easily pulled away from matrices, indicating a poor type of structure. The broken interface of matrix-altered specimens, on the other hand, has a coarser roughness because the nano-SiO_2 nanoparticles permeate into the matrices and adhere to the fiber surface. The existence of polymer fragments adhering to the fiber surface demonstrates the nanoparticles' contribution to improving the interface. The dispersion of nanoparticles inside the fibers and fiber–matrix interface is seen in SEM micrographs of matrix-altered specimens. As a result of the nanoparticles' inclusion in the matrices, the fiber and the matrix mechanical bonding are created. The inclusion of nanoparticles improves the matrix toughness in this way. The fragmented surface area of matrices-altered composite samples is bigger, which may lead to a higher interfacial fracture toughness rating.

Figure 7 shows SEM micrographs of Type II broken interfaces of baseline and matrices changed specimens (0.2, 0.4, and 0.6 wt% nano-SiO_2). Cracking or hackling can be seen on the delaminated faces. In matrices-edited specimens, the hackles are less noticeable. The appearance of epoxy-rich lumps from around the surface of the fiber indicates that the micro-SiO_2 deposition has cemented the fiber matrix altogether. Interfacial binding is stronger in the composite with 0.4 wt% SiO_2. The growth of hackles and the agglomerates of microcracks are slowed by better interaction. As a result, the composite rupture is delayed and the load is increased. The processes that mainly contribute to the Mode II interfacial toughness value include friction between the layer and hackles. At lower concentrations of micro-SiO_2, the contact between interfaces is insufficient to prevent the fracture from propagating. Cracks can easily propagate through softer resin-rich zones in certain circumstances, causing the composite to break quickly. The highest Type II interfacial fracture toughness scores were found in hemp composite materials with 0.4 wt% hemp.

4. Conclusion

This research focuses to see how adding nanoparticle fillers such as SiO_2 to hemp-reinforced polymer epoxy composites

affected the results. SiO_2 weight percentages of 0, 0.2, 0.4, and 0.6 were used. It is possible to have the following consequences:

(1) The findings showed that adding nanoparticles to the composite improved the Types I and II interfacial fractured toughness values significantly. The inclusion of nanofiller inclusions improved the composite's debonding resilience.

(2) Adding 0.4 wt% nano-SiO_2 to Types 1 and 2 increased the fracture value by 20.25% and 33.40%, respectively. The migration of nanoparticles into the surface of the fiber strengthened the fiber and the matrix interface while also improving the matrix's durability. The increased fiber and matrix interfacial binding was demonstrated via SEM pictures.

(3) The aggregates act as maximum stress points, causing the sample to fail at low stress. As a result, at greater weight percentages than 0.4 and 0.6 wt%, Types I and II interfacial fracture toughness values fall. The major effect of interface interaction among polymeric matrix, nanoparticles, and fiber reinforcement is responsible for the improved outcomes.

(4) The unfilled or empty specimen has a Type II interfacial fracture toughness value of 1,812 J/m^2. Among them, 0.4 wt% showed the greatest increase in values (2,721 J/m^2), increasing by 33.40%.

Data Availability

The data used to support the findings of this study are included within the article. Should further data or information be required, these are available from the corresponding author upon request.

Conflicts of Interest

The authors declare that they have no conflicts of interest.

Acknowledgments

The authors thank Saveetha School of Engineering, SIMATS, Chennai, for the technical assistance, and also appreciate the supports from Ambo University, Ethiopia.

References

[1] N. Svensson, R. Shishoo, and M. Gilchrist, "Manufacturing of thermoplastic composites from commingled yarns—a review," *Journal of Thermoplastic Composite Materials*, vol. 11, no. 1, pp. 22–56, 1998.

[2] C. S. Wu, Y. L. Liu, and Y. S. Chiu, "Epoxy resins possessing flame retardant elements from silicon incorporated epoxy compounds cured with phosphorus or nitrogen containing curing agents," *Polymer*, vol. 43, no. 15, pp. 4277–4284, 2002.

[3] I. Kyrikou and D. Briassoulis, "Biodegradation of agricultural plastic films: a critical review," *Journal of Polymers and the Environment*, vol. 15, pp. 125–150, 2007.

[4] G. Velmurugan and K. Babu, "Statistical analysis of mechanical properties of wood dust filled Jute fiber based hybrid composites under cryogenic atmosphere using Grey–Taguchi method," *Materials Research Express*, vol. 7, no. 6, Article ID 065310, 2020.

[5] M. Ponnusamy, L. Natrayan, S. Kaliappan, G. Velmurugan, and S. Thanappan, "Effectiveness of nanosilica on enhancing the mechanical and microstructure properties of kenaf/carbon fiber-reinforced epoxy-based nanocomposites," *Adsorption Science & Technology*, vol. 2022, Article ID 4268314, 10 pages, 2022.

[6] G. Velmurugan, M. A. S. Pasha, and V. Arasu, "Woven hemp and glass fiber hybrid composite—a comparative study on flexural and hardness properties with and without NaOH treatment," *International Journal of Pure and Applied Mathematics*, vol. 119, no. 10, pp. 1973–1978, 2018.

[7] V. Barbieri, M. L. Gualtieri, T. Manfredini, and C. Siligardi, "Lightweight concretes based on wheat husk and hemp hurd as bio-aggregates and modified magnesium oxysulfate binder: microstructure and technological performances," *Construction and Building Materials*, vol. 284, Article ID 122751, 2021.

[8] V. Ganesan and B. Kaliyamoorthy, "Utilization of Taguchi technique to enhance the interlaminar shear strength of wood dust filled woven jute fiber reinforced polyester composites in cryogenic environment," *Journal of Natural Fibers*, vol. 19, no. 6, pp. 1990–2001, 2022.

[9] E. Awwad, M. Mabsout, B. Hamad, M. T. Farran, and H. Khatib, "Studies on fiber-reinforced concrete using industrial hemp fibers," *Construction and Building Materials*, vol. 35, pp. 710–717, 2012.

[10] D. Asprone, M. Durante, A. Prota, and G. Manfredi, "Potential of structural pozzolanic matrix–hemp fiber grid composites," *Construction and Building Materials*, vol. 25, no. 6, pp. 2867–2874, 2011.

[11] G. Balčiūnas, S. Vėjelis, S. Vaitkus, and A. Kairytė, "Physical properties and structure of composite made by using hemp hurds and different binding materials," *Procedia Engineering*, vol. 57, pp. 159–166, 2013.

[12] L. Arnaud and E. Gourlay, "Experimental study of parameters influencing mechanical properties of hemp concretes," *Construction and Building Materials*, vol. 28, no. 1, pp. 50–56, 2012.

[13] F. P. La Mantia and M. Morreale, "Green composites: a brief review," *Composites Part A: Applied Science and Manufacturing*, vol. 42, no. 6, pp. 579–588, 2011.

[14] C. Ye, N. Hu, and Z. Wang, "Experimental investigation of *Luffa cylindrica* as a natural sorbent material for the removal of a cationic surfactant," *Journal of the Taiwan Institute of Chemical Engineers*, vol. 44, no. 1, pp. 74–80, 2013.

[15] H. Demir, U. Atikler, D. Balköse, and F. Tıhmınlıoğlu, "The effect of fiber surface treatments on the tensile and water sorption properties of polypropylene–luffa fiber composites," *Composites Part A: Applied Science and Manufacturing*, vol. 37, no. 3, pp. 447–456, 2006.

[16] C. Duan, N. Zhao, X. Yu, X. Zhang, and J. Xu, "Chemically modified kapok fiber for fast adsorption of Pb^{2+}, Cd^{2+}, Cu^{2+} from aqueous solution," *Cellulose*, vol. 20, pp. 849–860, 2013.

[17] J. Kazemi and V. Javanbakht, "Alginate beads impregnated with magnetic Chitosan@Zeolite nanocomposite for cationic methylene blue dye removal from aqueous solution," *International Journal of Biological Macromolecules*, vol. 154, pp. 1426–1437, 2020.

[18] N. Roy, K. Kannabiran, and A. Mukherjee, "Studies on photocatalytic removal of antibiotics, ciprofloxacin and

sulfamethoxazole, by Fe_3O_4–ZnO-Chitosan/Alginate nanocomposite in aqueous systems," *Advanced Powder Technology*, vol. 33, no. 8, Article ID 103691, 2022.

[19] H. Ismail, M. R. Edyham, and B. Wirjosentono, "Bamboo fibre filled natural rubber composites: the effects of filler loading and bonding agent," *Polymer Testing*, vol. 21, no. 2, pp. 139–144, 2002.

[20] J. Sarki, S. B. Hassan, V. S. Aigbodion, and J. E. Oghenevweta, "Potential of using coconut shell particle fillers in eco-composite materials," *Journal of Alloys and Compounds*, vol. 509, no. 5, pp. 2381–2385, 2011.

[21] M. T. Demirci, N. Tarakçıoğlu, A. Avcı, A. Akdemir, and İ. Demirci, "Fracture toughness (Mode I) characterization of SiO_2 nanoparticle filled basalt/epoxy filament wound composite ring with split-disk test method," *Composites Part B: Engineering*, vol. 119, pp. 114–124, 2017.

[22] M. Fernández-Álvarez, F. Velasco, A. Bautista, and B. Galiana, "Functionalizing organic powder coatings with nanoparticles through ball milling for wear applications," *Applied Surface Science*, vol. 513, Article ID 145834, 2020.

[23] Q. B. Guo, M. Z. Rong, G. L. Jia, K. T. Lau, and M. Q. Zhang, "Sliding wear performance of nano-SiO_2/short carbon fiber/epoxy hybrid composites," *Wear*, vol. 266, no. 7-8, pp. 658–665, 2009.

[24] M. Thangaraj, S. Arjunan, M. R. Krishnan, and P. S. Chelladurai, "Heat tolerant epoxy-amine functionalized graphene oxide composites for insulation applications," *Journal of Adhesion Science and Technology*, vol. 34, no. 16, pp. 1774–1795, 2020.

[25] L. P. Singh, D. Ali, and U. Sharma, "Studies on optimization of silica nanoparticles dosage in cementitious system," *Cement and Concrete Composites*, vol. 70, pp. 60–68, 2016.

[26] R. Liu, H. Xiao, H. Li et al., "Effects of nano-SiO_2 on the permeability-related properties of cement-based composites with different water/cement ratios," *Journal of Materials Science*, vol. 53, pp. 4974–4986, 2018.

[27] C. Zhuang and Y. Chen, "The effect of nano-SiO_2 on concrete properties: a review," *Nanotechnology Reviews*, vol. 8, no. 1, pp. 562–572, 2019.

[28] O. Akinyede, R. Mohan, A. Kelkar, and J. Sankar, "Static and fatigue behavior of epoxy/fiberglass composites hybridized with alumina nanoparticles," *Journal of Composite Materials*, vol. 43, no. 7, pp. 769–781, 2009.

[29] A. J. Kinloch, R. D. Mohammed, A. C. Taylor, S. Sprenger, and D. Egan, "The interlaminar toughness of carbon-fibre reinforced plastic composites using "hybrid-toughened" matrices," *Journal of Materials Science*, vol. 41, pp. 5043–5046, 2006.

[30] P. Rosso, L. Ye, K. Friedrich, and S. Sprenger, "A toughened epoxy resin by silica nanoparticle reinforcement," *Journal of Applied Polymer Science*, vol. 100, no. 3, pp. 1849–1855, 2006.

[31] S. Deng, L. Ye, and K. Friedrich, "Fracture behaviours of epoxy nanocomposites with nano-silica at low and elevated temperatures," *Journal of Materials Science*, vol. 42, pp. 2766–2774, 2007.

[32] Y. Tang, L. Ye, Z. Zhang, and K. Friedrich, "Interlaminar fracture toughness and CAI strength of fibre-reinforced composites with nanoparticles—a review," *Composites Science and Technology*, vol. 86, pp. 26–37, 2013.

[33] V. S. Shankar, G. Velmurugan, S. Kaliappan et al., "Optimization of CO_2 concentration on mortality of various stages of callosobruchus maculatus and development of controlled atmosphere storage structure for black gram grains," *Adsorption Science & Technology*, vol. 2022, Article ID 3381510, 12 pages, 2022.

[34] T. Manikandan, A. Siddharthan, R. Muruganandhan, and C. P. Sugumaran, "Influence of amine-functionalised graphene oxide filler on mechanical and insulating property of epoxy nanocomposites," *Materials Research Express*, vol. 6, no. 9, Article ID 095302, 2019.